

# Antagonistic activities of Klp10A and Orbit regulate spindle length, bipolarity and function in vivo

Joseph E. Laycock, Matthew S. Savoian\* and David M. Glover

Cancer Research UK Cell Cycle Genetics Group, University of Cambridge, Department of Genetics, Cambridge, CB2 3EH, UK

\*Author for correspondence (e-mail: MS476@mole.bio.cam.ac.uk)

Accepted 23 February 2006

Journal of Cell Science 119, 2354-2361 Published by The Company of Biologists 2006

doi:10.1242/jcs.02957

## Summary

The metaphase-spindle steady-state length occurs as spindle microtubules 'flux', incorporating new subunits at their plus ends, while simultaneously losing subunits from their minus ends. Orbit/Mast/CLASP is required for tubulin subunit addition at kinetochores, and several kinesins regulate spindle morphology and/or flux by serving as microtubule depolymerases. Here, we use RNA interference in S2 cells to examine the relationship between Orbit and the four predicted kinesin-type depolymerases encoded by the *Drosophila* genome (Klp10A, Klp59C, Klp59D and Klp67A). Single depletion of Orbit results in monopolar spindles, mitotic arrest and a subsequent increase in apoptotic cells. These phenotypes are rescued

by co-depleting Klp10A but none of the other three depolymerases. Spindle bipolarity is restored by preventing the spindle collapse seen in cells that lack Orbit, leading to functional spindles that are similar to controls in shape and length. We conclude that Klp10A exclusively antagonises Orbit in the regulation of bipolar spindle formation and maintenance.

Supplementary material available online at  
<http://jcs.biologists.org/cgi/content/full/119/11/2354/DC1>

Key words: Kinesin, Mitosis, Microtubule, Catastrophe factor, Flux, CLASP

## Introduction

In mitotic *Drosophila* cells the replicated centrosomes usually separate from one another around the intact prophase nuclear envelope. As this envelope becomes fenestrated at prometaphase onset, dynamic astral microtubules (MTs) nucleated from each of the opposing centrosomes invade the nuclear space where their plus-ends ultimately become attached to the sister kinetochores of each chromosome. Formation of these kinetochore MTs (kMTs) facilitates bipolar spindle formation and chromosome movement. After chromosome congression the spindle reaches a steady-state length, probably through the 'flux' of kMTs, whereby the incorporation of new tubulin subunits at the kinetochore is balanced by a simultaneous and equal loss at the spindle poles (Rogers et al., 2005). This state is maintained until the spindle-assembly checkpoint is satisfied and the cell enters into anaphase.

*Drosophila* Orbit/Mast (CLASP in vertebrates, hereafter referred to as Orbit) is a highly conserved microtubule-associated protein that stabilises microtubules (Inoue et al., 2000; Lemos et al., 2000; Akhmanova et al., 2001; Maiato et al., 2002; Maiato et al., 2003; Maiato et al., 2005). Mutations in *orbit* or RNA interference (RNAi) knockdown do not affect prophase centrosome separation but cause spindle collapse at flux-like velocities only after kMT formation during prometaphase (Maiato et al., 2002; Maiato et al., 2005). The kinetochores in such cells fail to remain associated with MT plus-ends and the chromosomes become buried in the centre of a monoaster causing a mitotic arrest (Maiato et al., 2002). The recent finding that Orbit is required for the incorporation of tubulin subunits at the

kinetochore for MT elongation and flux (Maiato et al., 2005) might therefore offer an explanation for the spindle collapse seen in Orbit-deficient cells.

The *Drosophila* genome encodes two families of putative kinesin-like protein (Klp) microtubule depolymerises, kinesin-8 and kinesin-13 (Lawrence et al., 2004), and members of each family have been implicated in regulating spindle morphology and/or flux. For example, depletion of Klp67A (kinesin-8) prevents proper centrosome separation and results in abnormally long, bipolar – yet monoastal – spindles (Goshima and Vale, 2003; Gandhi et al., 2004). The kinesin-13 family includes Klp10A, Klp59C and Klp59D. Both Klp10A and Klp59C have MT depolymerising activity in vitro and are required for proper chromosome movement in embryos. Klp10A localises transiently to centromeres but is spindle-pole- and/or centrosome-associated throughout mitosis where it is proposed to drive MT flux. The loss of Klp10A function causes a spindle collapse phenotype similar to that reported in Orbit-lacking cells. However, cells that lack functional Klp10A ultimately form bipolar spindles and enter anaphase (Goshima and Vale, 2003; Rogers et al., 2004).

Here, we investigate the interplay between Orbit and each of the four *Drosophila* Klp-type microtubule depolymerases using RNAi in S2 cells. We find that knockdown of Orbit alone results in monopolar spindles, mitotic arrest and subsequent apoptosis. Co-depletion with Klp10A was exclusively able to rescue spindle bipolarity allowing anaphase onset and cell-cycle progression, thereby diminishing the degree of apoptosis. We conclude that Orbit and Klp10A are an antagonistic MT-stabilising and -depolymerising pair that regulates spindle formation and morphology prior to entry into anaphase.

## Results

Knockdown of Klp10A but not of the other kinesin-type depolymerases moderates the amount of apoptosis in Orbit-deficient cells

To determine which, if any, of the kinesin-8 and/or kinesin-13 family members might counteract the activity of Orbit, we performed double RNAi depletion experiments for *orbit* combined with each of the four identified *Drosophila* Klp depolymerases in S2 cells. The effects of downregulation were initially assessed by flow cytometry 72 hours after treatment (Fig. 1). Depletion of Orbit alone (Fig. 1A) resulted in a significant increase in apoptotic cell debris as well as the proportion of 4N (G2-M) cells relative to 2N (G1), as expected from a mitotic delay followed by cell death. Simultaneous RNAi for *orbit* with either *Klp59C*, *Klp59D* or *Klp67A* showed no rescue of the proportions of cells of different ploidies in comparison to *orbit* knockdown alone, and the dual depletion with Klp67A dramatically increased the amount of cell death (supplementary material Fig. S1). By contrast, the single knockdown of Klp10A did not increase the number of apoptotic cells (Fig. 1B). Following double *orbit* and Klp10A RNAi (Fig. 1C), the proportion of 4N cells remained largely unchanged compared with the Orbit single downregulation, whereas that of 2N cells increased. This was associated with a marked diminution of apoptotic cells. Quantification of cells stained with Trypan Blue revealed that knockdown of *orbit* caused an approximately threefold increase in the number of apoptotic cells relative to controls (26.7% vs 8.7%). Co-depletion of Orbit and Klp10A reduced the proportion of dead cells to 14%. Together, these data suggest that the apoptosis associated with *orbit* RNAi can be selectively rescued by also depleting Klp10A but not other kinesin-type MT depolymerases.

## Bipolar and bi-centrosomal spindles form in cells depleted simultaneously but not individually of Orbit and Klp10A

Previous independent observations have revealed that Orbit and Klp10A regulate spindle microtubule dynamics. We therefore reasoned that the partial rescue seen in the FACS profiles of double depleted cells probably occurred during mitosis and examined spindle morphology in fixed cell populations. In cells treated with *orbit* double-stranded RNA (dsRNA) alone, the mitotic index rose from 4.4% to 14.5%. Almost all of the spindles in these cells were abnormal (93.4%;  $n=137$ ). Of these, 69% were monopolar with both centrosomes (as revealed by  $\gamma$ -tubulin staining) contacting one another at the centre of a large monoaster (Fig. 2B). Many of the remaining abnormal spindles were bipolar with a centrosome and aster capping each end, but were consistently shorter ( $6.46 \pm 0.13 \mu\text{m}$ ; range 4.35–9.78  $\mu\text{m}$ ;  $n=100$ ) than equally staged controls ( $7.60 \pm 0.16 \mu\text{m}$ ; range, 4.93–10.78  $\mu\text{m}$ ;  $n=100$ ; Fig. 2B',E).

Downregulation of Klp10A often led to monoastal but bipolar spindles upon which the majority of the chromosomes were equatorially positioned (Fig. 3C,C'). These spindles tended to be abnormally dense and significantly longer than their control counterparts (average length  $11.14 \pm 0.22 \mu\text{m}$ ; range 7.04–15.81  $\mu\text{m}$ ;  $n=100$ ; compare Fig. 2A,A' with C,C'). The mitotic index of Klp10A RNAi treated cells rose to 7.0%. This slight increase together with the detection of anaphase

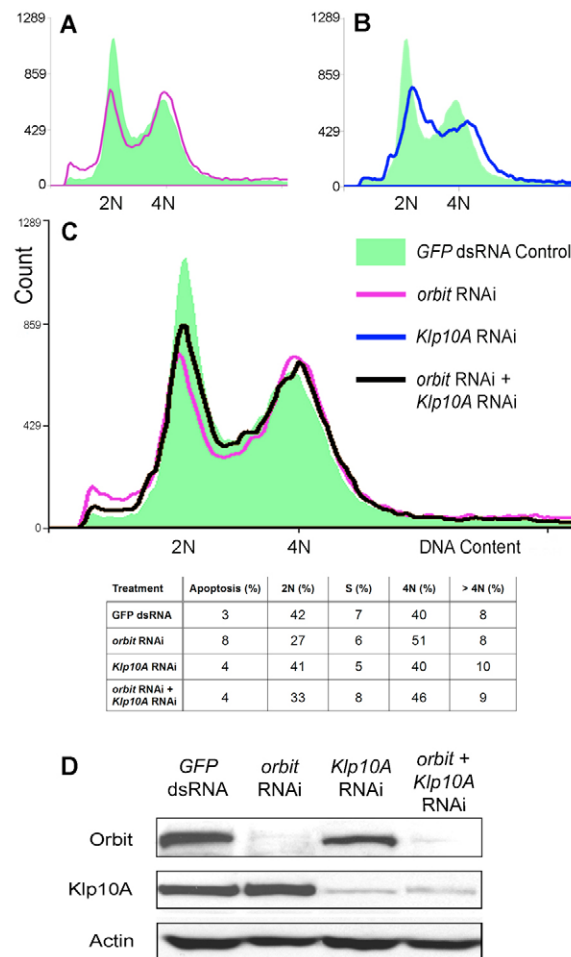


**Fig. 1.** RNAi of *Klp10A* diminishes the degree of apoptosis associated with Orbit depletion. (A) Knockdown of *orbit* alone (pink line) decreases the number of 2N cells while slightly increasing the number of presumptive mitotic cells with a 4N DNA content and dramatically increasing the number found in apoptosis relative to controls (solid green). (B) Klp10A downregulation (blue line) reduces the number of 2N cells while lowering and broadening the 4N peak, suggesting aneuploidy. (C) Double RNAi of *orbit* and *Klp10A* (black line) decreases the number of apoptotic cells seen following *orbit* RNAi as well as slightly increasing the proportion of 2N cells. Also shown are the relative distributions of cell population following each of the indicated treatments. (D) Western blot analysis of cell extracts taken from dsRNA-treated cells reveals substantial protein knockdown 72 hours after treatment. Actin is the loading control.

cells (data not shown) suggests that Klp10A depletion delays but does not prevent anaphase onset.

Double RNAi of *orbit* and *Klp10A* resulted in a mitotic index of 7.2%, a twofold decrease compared with *orbit* knockdown alone. Likewise, this decreased the number of abnormal mitotic cells from the 93.4% seen after *orbit* RNAi to 55.1% and the proportion of bipolar spindles rose from 31% to 62%. The average pole to pole distance of spindles in the double-RNAi-treated cells was  $7.59 \pm 0.18 \mu\text{m}$  (range 5.40–12.03  $\mu\text{m}$ ;  $n=100$ ), a value intermediate between the length of bipolar spindles following the individual knockdown experiments and one

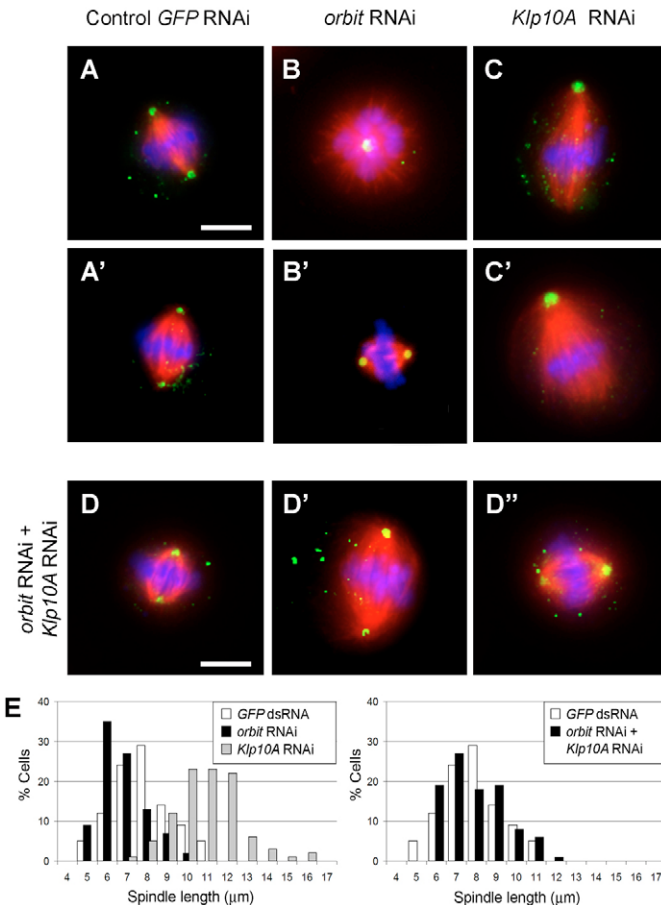


**Fig. 2.** Bipolar spindle morphology is restored in cells co-depleted of Orbit and Klp10A. (A–D'') Cells were treated with the indicated dsRNAs and stained for the distribution of microtubules ( $\alpha$ -tubulin; red),  $\gamma$ -tubulin (green) and DNA (blue) 72 hours later. (A,A') Control metaphase spindles are bipolar and bi-centrosomal with a centrosome (green) attached to each end. (B) *orbit* RNAi commonly results in monopolar spindles with both centrosomes at the centre of a monoaster. Bipolar spindles may form in Orbit depleted cells, although these tend to be abnormally short (B'). After *Klp10A* knockdown, spindles form that are on average about 150% the length of controls. Half of these spindles are marked by the presence of both centrosomes at a single, well focused, spindle pole and an acentrosomal pole that is focused to varying degrees (C,C'). Double RNAi against *orbit* and *Klp10A* rescues bipolar spindle morphology. These bipolar spindles can be placed in three classes: bipolar bi-centrosomal spindles morphologically similar to controls (D), bipolar bi-centrosomal spindles significantly longer than controls (D') and bipolar monoastrial spindles similar in length to controls but which have an asymmetric localisation of  $\gamma$ -tubulin. In this cell, the  $\gamma$ -tubulin diffusely stains one pole while at the other it forms a large aggregate in the centre of the aster, suggesting the presence of both centrosomes (D''), see text for details. (E) Distribution of spindle lengths following each of the indicated treatments. Note the enhancement of spindle length in *Klp10A* single downregulated cells and the shortening of those in cells depleted of Orbit. The double knockdown of *orbit* and *Klp10A* can rescue the average spindle length and further restores the distribution of spindle lengths to values similar to that seen in the controls. All images are shown at the same magnification. Bars, 10  $\mu$ m.

indistinguishable from that seen in control cells (compare with  $7.60 \pm 0.16$   $\mu$ m; Fig. 2E). Based on morphology, the bipolar spindles were placed into three classes. In the first and most prevalent group (36 of 100 spindles), shown in Fig. 2D, spindles were of normal length and capped on each end by a centrosome. Spindles of the second class also had centrosomes at each pole but were reminiscent of those seen following *Klp10A* RNAi alone and tended to be abnormally long (15% of spindles; Fig. 2D'). The third class of bipolar spindle was observed in 30% of all cells analysed and was similar in shape and length to controls, but had an asymmetrical distribution of  $\gamma$ -tubulin at the two poles, suggestive of unequal numbers of centrosomes or as represented in Fig. 2D'', two centrosomes at one pole and spindle-associated  $\gamma$ -tubulin at the other. From these observations we conclude that double *orbit* and *Klp10A* downregulation restores spindle bipolarity and function.

#### Spindle bipolarity and mitotic progression are rescued in double-depleted cells by preventing prometaphase spindle collapse

Single depletions of either Orbit or Klp10A have been shown to cause spindle collapse shortly after prometaphase onset leading, at least transiently, to the formation of monopolar spindles. This raises the possibility that the bipolar spindles seen in double-RNAi cells could arise either through the prevention of the collapse or through a re-separation of the centrosomes after it. To differentiate between these mechanisms, GFP- $\alpha$ -tubulin-expressing S2 cells were followed by time-lapse imaging after downregulating Orbit and Klp10A individually or together.

As represented in Fig. 3A, the centrosomes in control cells were independent during prophase and either continued to separate or maintained relative separation during spindle formation (0–400 seconds; see also Fig. 4C and supplementary material Movie 1). Following chromosome alignment, as revealed by a non-fluorescent equatorial 'shadow', the spindle shortened slightly and assumed a length of about 7  $\mu$ m (1480 seconds). Approximately 15 minutes later this cell entered anaphase (2180 seconds). The duration of prometaphase in control cells, i.e. the time from the initiation of spindle formation to anaphase onset, was  $30.4 \pm 2.7$  minutes ( $n=19$ ).

In all of the *orbit*-RNAi-treated cells filmed ( $n=13$ ), the centrosomes were separated from one another during prophase. In 85% (11 of 13) of these cells the centrosomes began to collapse towards one another to form a monoaster after a nascent bipolar spindle was detected (Fig. 3B; 0–900 seconds, Fig. 4C, supplementary material Movie 2). In several cells transient multipolar spindles formed as bundles of MTs became focused distal to the monoaster (Fig. 3B; 1260s arrowheads). These 'mini-spindles' were unstable and could change configuration (Fig. 3B; 1770s arrowhead). None of these 11 cells entered into anaphase during the 200-minute filming period. Furthermore the centrosomes never separated from one another after their initial collapse. In a few (two of 13) instances short, bipolar spindles formed resembling those seen in our fixed-cell studies. Despite the reduced separation between the centrosomes, these cells underwent anaphase and exited mitosis.

We found that the centrosomes also collapsed together during prometaphase to form transient monopolar spindles in 50% of the cells treated with *Klp10A* dsRNA ( $n=20$ ) (Fig. 3C;

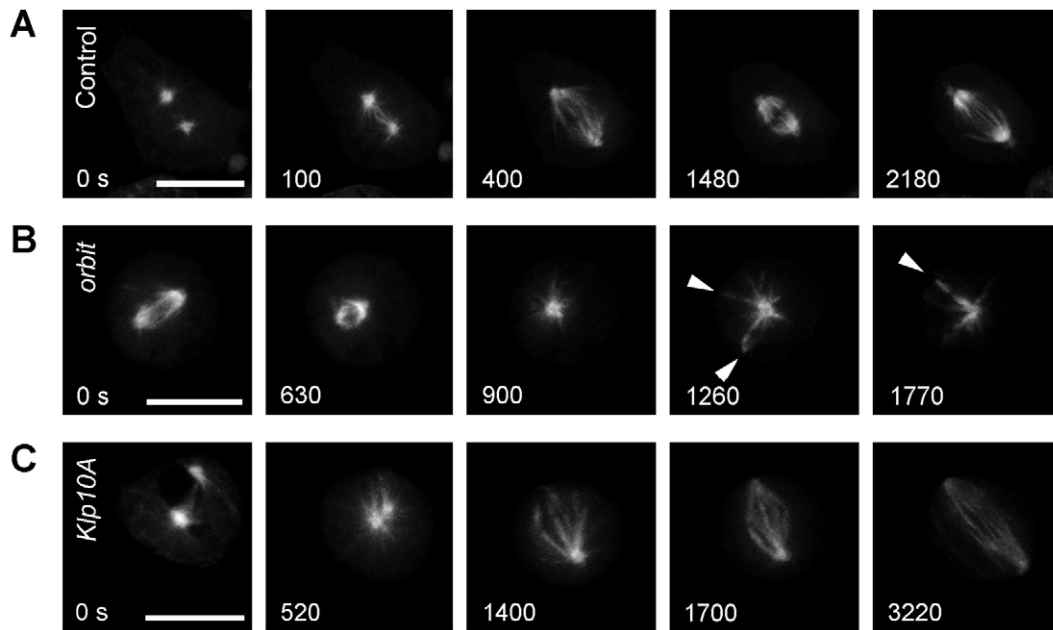


**Fig. 3.** Spindle formation in living S2 cells expressing GFP-tubulin after *orbit* or *Klp10A* RNAi. Selected frames from time-lapse sequences showing spindle formation and mitotic progression in (A) control, (B) *orbit* RNAi- and (C) *Klp10A* RNAi-treated cells. (A) In control cells the two separated centrosomes oppose one another on the nuclear envelope during prophase. At prometaphase onset (0 s) the nuclear envelope becomes fenestrated and astral MTs interact with the kinetochores to form a bipolar spindle (100) that becomes more robust as the chromosomes congress to the equatorially positioned metaphase plate (400), the fluorescence ‘shadow’ at the equator indicates the presence of the chromosomes. The spindle in this cell slightly shortens at metaphase (1480) after assuming a steady state length which it maintains until anaphase onset (2180) (see also supplementary material Movie 1). (B) *orbit* RNAi does not prevent prophase centrosome separation. As the chromosomes become bi-oriented during prometaphase, the nascent bipolar spindle collapses upon itself (0–630 seconds) to form a monopolar spindle (900). In this cell, transient multi-poles (1260–1770 seconds; arrowheads) form that are probably generated by individual or small clusters of chromosomes as evidenced by the shadow at their equators (see text for details). (C) Knockdown of *Klp10A* does not perturb the initial separation of the centrosomes at prophase but, as illustrated here, causes their subsequent collapse during prometaphase in 50% of the cells followed by time-lapse microscopy (0–520 s). Unlike *Orbit*-depleted cells, those lacking *Klp10A* are able to form stable bipolar spindles (1400–1700 seconds) that are monoastral. These spindles are fully functional and cells can enter into anaphase (3220). Time (in brackets) is in seconds relative to prometaphase onset. Bars, 10  $\mu$ m (see also supplementary material Movie 2).

0 seconds, 520 seconds; Fig. 4C and supplementary material Movie 2). In the cell shown in Fig. 3C, the single monoaster then extended to form a centrosome-free spindle pole distal to the first and generated a monoastral bipolar spindle (Fig. 3C; 1400, 1700s). Such monoastral bipolar spindles required  $39.2 \pm 3.6$  minutes ( $n=10$ ) to advance from prometaphase into anaphase. It is noteworthy that when *Klp10A*-depleted cells entered anaphase and cytokinesis they formed atrophied and abnormally long central spindles and intracellular bridges (data not shown).

As illustrated in Fig. 4, in contrast to the spindle collapse we observed in the cells following *orbit* or *Klp10A* RNAi alone, in most cells depleted of both proteins the centrosomes remained separated beyond prophase and formed a stable bipolar spindle. We found that 14 of 20 cells maintained or increased their centrosome separation distance after prometaphase onset and formed bipolar and bi-astral spindles. Despite forming bipolar spindles with kinetics similar to controls, double-knockdown cells were often delayed in entering anaphase. Unlike control cells, in which prometaphase lasted about 30 minutes, only six of 14 double-RNAi-treated cells entered anaphase within 45 minutes of spindle formation (Fig. 4A, supplementary material Movie 3)

and the remaining eight cells did not enter into anaphase within 65 minutes. Because our FACS data indicated that *orbit* and *Klp10A* double-RNAi cells reduced the frequency of apoptosis seen following *orbit* knockdown alone, we reasoned that although they undergo a prolonged prometaphase, these double-depleted cells were not permanently arrested. We therefore repeated our time-lapse experiments and followed 14 cells for up to 200 minutes, an interval 6.5 times greater than that required for control cells to enter anaphase. Of these 14 cells filmed, three failed to form bipolar spindles and did not advance into anaphase during the course of filming. Of the remaining 11 cells that formed bipolar spindles, two entered anaphase within about 30 minutes of prometaphase onset. Another three cells progressed into anaphase within 45 minutes, whereas the remaining six cells required between 74 and 147 minutes for anaphase onset (Fig. 4B, supplementary material Movie 3). These live cell studies indicate that the simultaneous RNAi of *Klp10A* and *orbit* prevents the centrosome-collapse phenotype observed in single knockdown cells. The resulting bipolar spindles are functional enough to promote chromosome congression and anaphase onset, although the timing of this latter event can be substantially delayed.



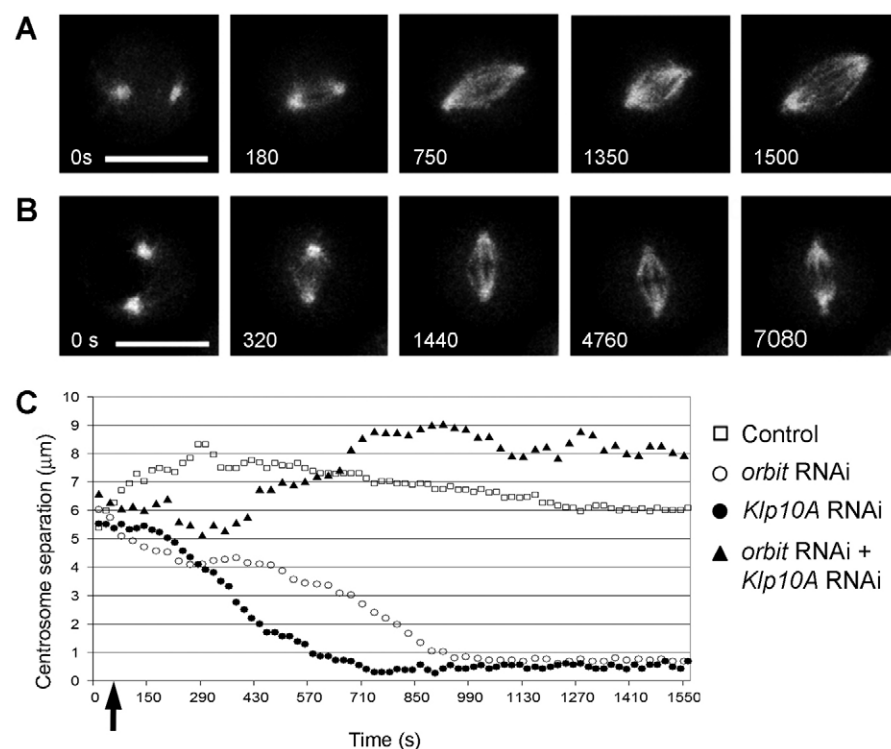


**Fig. 4.** Time-lapse imaging reveals that simultaneous RNAi of *orbit* and *Klp10A* rescues spindle bipolarity by preventing spindle collapse. (A,B) Selected frames from time-lapse sequences of cells depleted of both Orbit and Klp10A. Time is in seconds relative to prometaphase onset. Unlike in cells downregulated for either Orbit or Klp10A alone, the separation distance between the centrosomes at prophase remains constant or increases during spindle formation. Note the large variation in time needed for anaphase onset between the double-knockdown cells. See text for details. (C) Kinetic profiles of centrosome separation for the cells shown in Fig. 3 and Fig. 4A. Prometaphase onset occurs at 0 seconds. Bars, 10  $\mu\text{m}$ .

#### The delay in anaphase onset seen in *orbit* and *Klp10A* double-RNAi cells correlates with decreased centromeric tension and BubR1 retention

Our fixed and live cell observations indicated that the chromosomes in *orbit* and *Klp10A* double-downregulated cells reached an equatorial position with the same frequency as control cells. Since chromosome congression is a hallmark of attachment, we investigated whether the kinetochores are under tension, the absence of which could account for the delayed anaphase entry (Taylor et al., 2004; Tan et al., 2005). We therefore measured the distance between sister centromeres as revealed by CID (centromere identifier), the *Drosophila* equivalent of modified histone CENP-A (Blower and Karpen, 2001) (Fig. 5A,B). In control prophase cells the average intra-centromeric distance was  $0.63 \pm 0.01 \mu\text{m}$  ( $n=35$ ). Since this period is prior to spindle attachment, this is the relaxed or resting separation distance. After bi-orientation and metaphase alignment the separation was  $0.96 \pm 0.02 \mu\text{m}$  ( $n=81$ ), which we define as the tensed state.

We carried out similar measurements following RNAi against *orbit* and *Klp10A* either individually or simultaneously (Fig. 5A,B). In Orbit-depleted cells that formed monopolar spindles the average intra-centromeric distance was  $0.72 \pm 0.01 \mu\text{m}$  ( $n=92$ ), consistent with a lack of bi-orientation. This value increased to  $0.94 \pm 0.04 \mu\text{m}$  ( $n=43$ ) when the chromosomes attached to either transient multipolar or short bipolar spindles. The average centromeric separation distance after *Klp10A* RNAi varied according to spindle morphology and for monoastal bipolar spindles was  $0.87 \pm 0.03 \mu\text{m}$  ( $n=70$ ). Surprisingly, this distance rose by 73% to  $1.20 \pm 0.03 \mu\text{m}$  ( $n=93$ ) when the chromosomes had congressed upon bipolar spindles that had an aster at each end. A similar, but lesser, trend was observed in cells that were RNAi-treated for both

*orbit* and *Klp10A*. The average intra-centromeric distance of chromosomes on bipolar, monoastal spindles in these cells was  $0.80 \pm 0.02 \mu\text{m}$  ( $n=50$ ), whereas those on bipolar spindles capped at each pole by a centrosome and aster was  $0.86 \pm 0.01 \mu\text{m}$  ( $n=110$ ). These average values are less than tensed controls and, moreover, the double-knockdown population had a distribution of distances with a greater proportion of the centromeres under less tension than that observed in the controls (Fig. 5B).

We next examined the localisation of the tension-sensitive BubR1 checkpoint protein (Logarinho et al., 2004; Howell et al., 2004) in control and knockdown cells. As shown in Fig. 5C, in control cells BubR1 was detected as a faint signal on the kinetochores of chromosomes that had congressed to the spindle equator. Equatorially positioned chromosomes in *Klp10A* RNAi cells similarly lacked BubR1, whereas intensely staining punctae could be detected within the same cell on chromosomes adjacent to the spindle poles, which are presumably mono-oriented and not under tension. BubR1 was seen as multiple spots on the chromosomes buried in the monoasters of Orbit-lacking cells, but like with control metaphase cells, this signal intensity was reduced for equatorially positioned chromosomes on bi- or multi-polar spindles. As illustrated in Fig. 5C, we found that BubR1 staining intensity appeared higher on the kinetochores of congressed chromosomes of *orbit* and *Klp10A* double-knockdown cells than in controls and that this signal intensity could vary between adjacent chromosomes. From these data we conclude that the bipolar spindles in cells lacking Orbit and Klp10A interact with the kinetochores to generate tension. The amount of tension is less than that observed in the controls correlating with the retention of the BubR1 checkpoint protein on kinetochores and delayed anaphase entry.

## Discussion

Bipolar spindle formation and maintenance occur through the actions of multiple motor and microtubule dynamics-altering proteins (Sharp et al., 2000). Here, we examined the interplay between Orbit, a protein needed for tubulin-dimer incorporation into kinetochore MTs, and each of the four microtubule depolymerising kinesins Klp67A, Klp10A, Klp59C and Klp59D. We found that the co-depletion of Klp10A but not of the other KLP MT depolymerases diminished the number of apoptotic cells and prevented the spindle collapse associated with *orbit* knockdown. In contrast to individual downregulation of Orbit or Klp10A that resulted in abnormally short and/or monopolar or long spindles, respectively, spindles in double-deficient cells were bipolar and of an average length indistinguishable from controls. These spindles promoted chromosome alignment and anaphase entry,

indicating that they were functional. Since both Orbit and Klp10A have been directly implicated in microtubule flux (Rogers et al., 2004; Maiato et al., 2005), these data suggest that this process is not required to determine mitotic spindle morphology or chromosome congression in *Drosophila* tissue culture cells.

During the course of this work, it was reported that microtubule flux is not essential for bipolar spindle formation and chromosome congression in mitotic vertebrate cells (Ganem et al., 2005). In contrast to the knocked down MT-stabilising and -depolymerising protein pair described here, the experiments by Ganem et al. (Ganem et al., 2005) used the co-depletion of two kinesin-13 depolymerases: Kif2A, the orthologue of Klp10A and Kif2C/MCAK/XKCM1, the vertebrate counterpart of Klp59C. Both Kif2A and Kif2C have overlapping localisations at centromeres and spindle poles

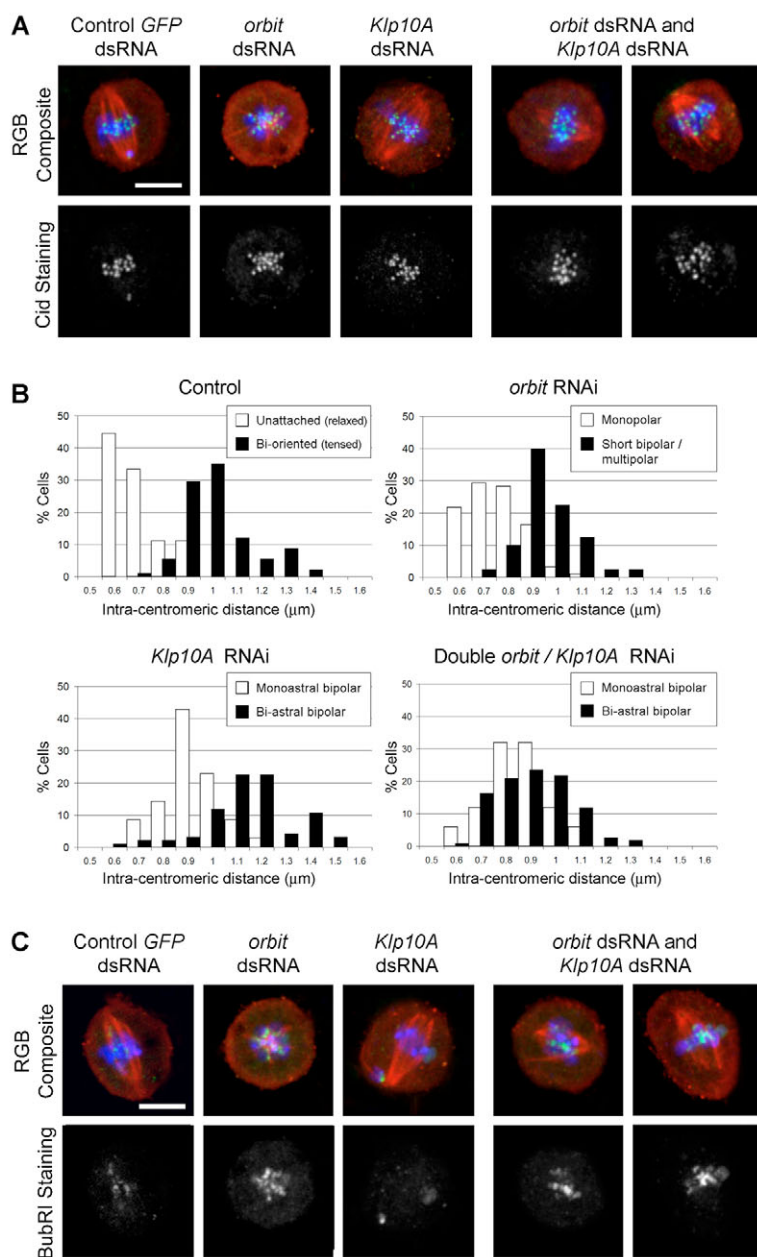


**Fig. 5.** Double *orbit*- and *Klp10A*-depleted cells have reduced intra-centromeric tension and retain BubR1 at their kinetochores. S2 cells were treated with dsRNA for 72 hours before being fixed and stained to localise microtubules ( $\alpha$ -tubulin; red), DNA (blue) and, in green, either CID (A) or BubR1 (C). (A) Chromosome configurations representing the different classes measured are shown. (B) Distributions of intra-centromeric distances under each of the indicated conditions. Following bi-orientation in control cells, metaphase centromeres are placed under tension as revealed by the increased intra-centromeric distances relative to unattached 'relaxed' prophase centromeres. Knockdown of *Klp10A* and *orbit*, either singly or simultaneously, alters the degree of centromeric separation. Note how the distributions and magnitudes of the separation distances increase when spindles are capped on both ends by an aster, compared with bipolar spindles with an aster at only one end. Even when placed on bi-astral, bipolar spindles, the centromeres in double-knockdown cells are under less tension than those in controls. See text for details. (C) BubR1 localisation correlates with spindle morphology and chromosome position. In control metaphase cells, BubR1 is seen as a few faint punctae. By contrast, in *orbit* knockdown cells that form monopolar spindles, the staining intensity at kinetochores is markedly increased, consistent with a failure to bi-orient and lack of tension. Downregulation of *Klp10A* does not prevent bipolar spindle formation, chromosome bi-orientation or congression. As with controls, equatorially positioned chromosomes in these cells show little BubR1 staining, whereas those that are lagging at the spindle pole and are presumably mono-oriented exhibit a robust signal. Equatorially positioned chromosomes in *orbit* and *Klp10A* double-RNAi cells display intense BubR1 staining on some kinetochores but not others. Bars, 5  $\mu$ m.

and/or centrosomes (e.g. Kline-Smith and Walczak, 2002; Gaetz and Kapoor, 2004; Ganem and Compton, 2004) and loss of either leads to a prometaphase spindle collapse (Kline-Smith and Walczak, 2002; Ganem and Compton, 2004). This monopolar spindle phenotype was rescued by simultaneously depleting both of these MT depolymerases (Ganem and Compton, 2004), suggesting they form an antagonistic pair. However, an orthologous antagonism of Klp10A and Klp59C does not exist during mitosis in *Drosophila*, because loss of Klp59C function in tissue culture cells (Goshima and Vale, 2003) or syncytial embryos (Rogers et al., 2004) does not alter spindle morphology, and dual perturbations result in spindle abnormalities identical to that observed following single Klp10A disruptions (Rogers et al., 2004).

We propose that bipolar spindle formation occurs in at least two phases. During the first, MTs nucleated from the separated centrosomes invade the nuclear volume and make their initial interactions with the kinetochores. Time-lapse analyses indicate that this step is not affected by the depletion of either Orbit or Klp10A (Maiato et al., 2002; Maiato et al., 2005; Goshima and Vale, 2003) (this study) and is thus Orbit- and Klp10A-independent. The second phase, spindle stabilisation, occurs after chromosome bi-orientation and probably results from antagonistic pairs of molecules regulating the dynamics of the plus- and minus-ends of kinetochore MTs. It is at this stage that Orbit and Klp10A become engaged as evidenced by the collapse of the nascent spindle following their individual perturbations (e.g. Maiato et al., 2002; Maiato et al., 2005; Goshima and Vale, 2003) (this study). Although we cannot rule out the possibility that the spindle collapse results from a loss of interpolar MT integrity, we feel this is unlikely. First, because the rate at which spindles collapse after *orbit* RNAi is similar to the rate of MT flux in *Drosophila* tissue culture cells (compare 0.7  $\mu\text{m}/\text{minute}$  with  $\sim 0.6 \mu\text{m}/\text{minute}$  for each half spindle) (Maiato et al., 2002; Maiato et al., 2005), consistent with a flux depolymerase shortening kMTs in the absence of new tubulin-polymer growth at the kinetochore. Second, because kMTs that form independently from the centrosome and primary spindle axis (i.e. a mini-spindle) also shrink in the absence of Orbit (Maiato et al., 2005). Since these bundles of kMTs are not present between two half spindles it unlikely that their shortening is the result of intervening interpolar MTs. Likewise, it has been previously demonstrated that the spindle collapse associated with the loss of Kif2A is kMT-dependent. Spindle bipolarity was restored in these cells by co-depleting the Nuf2 kinetochore protein, thereby preventing kMT formation without affecting any other spindle MTs (Ganem and Compton, 2004). In the case of Orbit and Klp10A single-depleted cells, we envisage that the spindle collapse is due to an imbalance of regulatory components following the activation of the flux machinery during this second phase. Collapse could result, for example, as Klp10A depolymerises the non-polymerising kMTs that result from *orbit* downregulation. Conversely, because flux-generated tension has been proposed to promote tubulin subunit incorporation at kinetochores (Maddox et al., 2003), depletion of Klp10A could also affect polymerisation of kMTs, which – in the presence of other active phase two depolymerases – would cause spindle collapse. In the absence of Orbit and Klp10A the flux machinery would not become engaged and spindle length would be determined by other antagonistic molecular pairs.

Our data in flies, in concert with that found in vertebrates, indicate that although microtubule flux is a characteristic of many animal cells it is not essential for pre-anaphase chromosome movements or spindle formation. Nevertheless, the plasticity it imparts is probably advantageous for spindle and kinetochore interactions, for example by promoting kMT polymerisation (Maddox et al., 2003) or by generating tension for satisfying the spindle checkpoint. We found that cells simultaneously depleted of Klp10A and Orbit tended to spend variable but extremely prolonged periods of time in mitosis before entering anaphase. Since both our fixed and live cell studies did not reveal an increase in non-equatorially positioned chromosomes compared with controls, we believe that the prometaphase arrest was not due to activation of the checkpoint through unattached kinetochores. Although never fully relaxed, the centromeres of bi-oriented chromosomes in double-knockdown cells tended to be under diminished tension relative to controls. This corresponded to the retention of BubR1 at kinetochores. Cells depleted only of Klp10A also spent more time in prometaphase than their control counterparts (Goshima and Vale, 2003) (this study), although this duration was substantially less than that observed for *orbit* and Klp10A double-RNAi cells. Despite decreased intra-centromeric tension in Klp10A downregulated cells, we did not observe BubR1 on the kinetochores of congressed chromosomes. One explanation for this is that, even without flux, spindle MTs can still produce tension by transducing cortical forces. Here, the long spindles that form in the absence of Klp10A would position the asters in direct contact with the cortex where their component MTs would make increased numbers of contacts with cortical motor proteins such as cytoplasmic dynein. Just as cortex-based forces by this motor act along astral MTs for spindle positioning (Dujardin and Vallee, 2002), astral pulling could generate tension across the centromeres and kinetochores of congressed chromosomes. If true, centromeric tension should correlate with the presence or absence of asters. We found this to be the case, and sister centromeres were separated to a greater extent when they were on bi-astral spindles than when attached to bipolar spindles with a single aster (Fig. 5B). Moreover, in those Klp10A-depleted cells displaying bipolar spindles capped at each end by an overgrown aster, the average intra-centromeric distance was greater than that seen in the controls.

Together, our observations indicate that Orbit and Klp10A are an antagonistic molecular pair, consistent with their previous individual implicated roles in MT flux, a process we show here to be dispensable for bipolar spindle formation and chromosome congression. Our data further suggest that astral-mediated pulling forces are involved in checkpoint satisfaction. To our knowledge, the role that these forces may serve in the checkpoint has not been previously reported and thus merits further investigation.

## Materials and Methods

### Cell culture

*Drosophila* S2 cells were cultured in Schneider insect medium supplemented with 10% foetal calf serum (FCS) and penicillin-streptomycin. S2 cells expressing GFP- $\alpha$ -tubulin (Goshima and Vale, 2003) were grown in the same medium supplemented with 100  $\mu\text{g}/\text{ml}$  hygromycin B.

### RNAi-mediated protein depletion

The following double-stranded RNAs (dsRNAs) were used: Orbit (against basepairs 1685–2193, using primers 5'-CCCGATTGGCCGAACACCTGGAACC-3' and 5'-



ACGTCGAGACCCCGCACCTGTAGAGT-3', corresponding to the MT-binding domain), Klp59C, Klp59D (see Rogers et al., 2004), Klp10A (against the first 880 bp of the longest open reading frame, using the primers 5'-ATGGACATGATTACGGTG-3' and 5'-CATCGATCTCCTTGCGATT-3', which terminates before the predicted motor domain sequence) and Klp67A (against basepairs 1050-1851, using the primers 5'-GAAACAGAATGTCTCAAGT-3' and 5'-GCTGCTGCGCAGAGCCACAG-3', corresponding to a region beyond that predicted to encode the motor domain). For each reaction 20 µg of dsRNA was transfected into S2 tissue culture cells with Transfast (Promega) and observed 72 hours later. For control reactions either dsRNA against GFP (primers 5'-CTTCAGCCGCTACCCC-3' and 5'-TGTCGGGACGACG-3') or Transfast alone was used and gave similar results.

### FACs analysis, Trypan Blue staining and western blots

The cell-cycle profiles of S2 cell samples were analysed using a Becton Dickinson LSR cytometer, with 30,000 events recorded per sample. Propidium iodide fluorescence, pulse-width, forward scatter and side-scatter were measured. To determine the ratios of each cell population FACs profiles were imported into the DakoCytomation Summit software. The areas of the apoptotic, 2N and 4N peaks were derived by using a best-fit curve that was symmetrical around a midline corresponding to each peak's maxima. The percentages of cells in S phase were calculated by subtracting the 2N and 4N peaks from a total 2N-4N gate. The remaining cells are denoted as polyploid. To determine apoptotic frequency of non-suspended cells, 10 µl of Trypan Blue solution (0.4%) (Sigma) was added to 90 µl of re-suspended cell sample. Duplicate samples were scored in cells using a Neubauer haemocytometer. The trends following each treatment are similar, even though the exact proportions of apoptotic cells scored varies between these different techniques, suggesting that the variations result from differences in the sensitivities of each method. Standard western blotting techniques were used and membranes were probed with the following antibodies and dilutions; anti-Orbit (Inoue et al., 2004) (1:2000), a rabbit polyclonal raised against the approximately the first 215 residues of Klp10A (M.S.S. and D.M.G. unpublished; 1:2000), anti-actin (Sigma; 1:2000). Appropriate secondary antibodies were visualised by using the ECL system.

### Immunofluorescence and data analysis

Samples were pre-extracted for 1 minute in PHEM (60 mM PIPES, 25 mM HEPES, 10 mM EGTA, 4 mM MgSO<sub>4</sub>) containing 1% Tween 20, and then fixed in 3.7% formaldehyde for 10 minutes. Samples were blocked for 1 hour in PBS containing 5% BSA and 1% Triton X-100. Cells were incubated overnight at 4°C in primary antibodies diluted in blocking solution to the following concentrations: Klp10A 1:200, α-tubulin (YL1/2; Oxford Biotechnology) 1:50, γ-tubulin (GTU488; Sigma) 1:100, CID (AbCAM) 1:200 and BubR1 (a kind gift of C. Sunkel, Institute of Molecular and Cellular Biology, University of Porto, Portugal) 1:200. Commercially available secondary antibodies were used and DNA was stained with either ToTo3 or DAPI.

Fluorescence images were acquired on either a Nikon Optiphot microscope fitted with a Biorad scanning confocal head or a Zeiss Axiovert200 widefield fluorescence microscope, each using a 100× (N.A. 1.4) lens. Images shown are the maximum-intensity projections of a variable number of z-sections collected at 0.25 µm intervals and processed in Photoshop (Adobe Photo Systems).

All measurements were performed with Metamorph (Universal Imaging). To avoid bias in our analysis by only using spindles that retained a centrosome at each pole, spindle lengths were determined by measuring the distance between the focused spindle poles as revealed in maximum-intensity projections. To evaluate the tension state of the kinetochores, the separation distance between co-planar, paired CID spots, which correspond to sister centromeres, was measured. Values were then exported into Microsoft Excel for plotting.

### Time-lapse microscopy

GFP-tubulin-expressing cells were filmed 3 days after being treated with dsRNA. Cells in this line often contain supernumerary centrosomes (Goshima and Vale, 2003), a characteristic that was not amenable to our current study. We therefore optically sectioned each cell of interest both before and during the course of filming to allow detection of ectopic centrosomes and removed those cells from the data set. z-sectioning was further necessary to follow MT behaviour as we chose not to artificially flatten our cells with reagents such as concanavilin A, which might influence spindle formation. Cells grown on coverslips were mounted in a POC-R chamber (Zeiss) and maintained in supplemented Schneider insect media at 25°C by using a Tempcontrol 37-2, stage- and objective-lens-heating system (Zeiss). Cells were imaged with a Perkin Elmer Ultraview RSIII spinning disk confocal head mounted on a Zeiss Axiovert200 microscope with a 100× (N.A. 1.4) lens and a 2×2 bin. At 20- to 30-second intervals z-series consisting of no more than seven 1-µm steps were acquired.

We thank E. Mathe for aid in the generating the Klp10A antibody. This work was made by possible grants to D.M.G. from the Cancer Research UK and Medical Research Council, and a studentship from the Biotechnology and Biological Sciences Research Council.

### References

- Akhmanova, A., Hoogenraad, C. C., Drabek, K., Stepanova, T., Dortland, B., Verkerk, T., Vermeulen, W., Burgering, B. M., De Zeeuw, C. I., Grosveld, F. et al. (2001). CLASPs are CLIP-115 and -170 associating proteins involved in the regional regulation of microtubule dynamics in motile fibroblasts. *Cell* **104**, 923-935.
- Blower, M. D. and Karpen, G. H. (2001). The role of *Drosophila* CID in kinetochore formation, cell-cycle progression and heterochromatin interactions. *Nat. Cell Biol.* **3**, 730-739.
- Dujardin, D. L. and Vallee, R. B. (2002). Dynein at the cortex. *Curr. Opin. Cell Biol.* **14**, 44-49.
- Gaetz, J. and Kapoor, T. M. (2004). Dynein/dynactin regulate metaphase spindle length by targeting depolymerizing activities to spindle poles. *J. Cell Biol.* **166**, 465-471.
- Gandhi, R., Bonaccorsi, S., Wentworth, D., Doherty, S., Gatti, M. and Pereira, A. (2004). The *Drosophila* kinesin-like protein KLP67A is essential for mitotic and male meiotic spindle assembly. *Mol. Biol. Cell* **15**, 121-131.
- Ganem, N. J. and Compton, D. A. (2004). The Kif1 kinesin Kif2a is required for bipolar spindle assembly through a functional relationship with MCAK. *J. Cell Biol.* **166**, 473-478.
- Ganem, N. J., Upton, K. and Compton, D. A. (2005). Efficient mitosis in human cells lacking poleward microtubule flux. *Curr. Biol.* **15**, 1827-1832.
- Goshima, G. and Vale, R. D. (2003). The roles of microtubule-based motor proteins in mitosis: comprehensive RNAi analysis in the *Drosophila* S2 cell line. *J. Cell Biol.* **162**, 1003-1016.
- Howell, B. J., Moree, B., Farrar, E. M., Stewart, S., Fang, G. and Salmon, E. D. (2004). Spindle checkpoint protein dynamics at kinetochores in living cells. *Curr. Biol.* **14**, 953-964.
- Inoue, Y. H., do Carmo Avides, M., Shiraki, M., Deak, P., Yamaguchi, M., Nishimoto, Y., Matsukage, A. and Glover, D. M. (2000). Orbit, a novel microtubule-associated protein essential for mitosis in *Drosophila melanogaster*. *J. Cell Biol.* **149**, 153-166.
- Inoue, Y. H., Savoian, M. S., Suzuki, T., Mathe, E., Yamamoto, M. T. and Glover, D. M. (2004). Mutations in orbit/mast reveal that the central spindle is comprised of two microtubule populations, those that initiate cleavage and those that propagate furrow ingression. *J. Cell Biol.* **166**, 49-60.
- Kline-Smith, S. L. and Walczak, C. E. (2002). The microtubule-destabilizing kinesin XKCM1 regulates microtubule dynamic instability in cells. *Mol. Biol. Cell.* **13**, 2718-2731.
- Lawrence, C. J., Dawe, R. K., Christie, K. R., Cleveland, D. W., Dawson, S. C., Endow, S. A., Goldstein, L. S., Goodson, H. V., Hirokawa, N., Howard, J. et al. (2004). A standardized kinesin nomenclature. *J. Cell Biol.* **167**, 19-22.
- Lemos, C. L., Sampaio, P., Maiato, H., Costa, M., Omelyanchuk, L. V., Liberal, V. and Sunkel, C. E. (2000). MAST, a conserved microtubule-associated protein required for bipolar mitotic spindle localisation. *EMBO J.* **19**, 3668-3682.
- Logarinho, E., Bousbaa, H., Dias, J. M., Lopes, C., Amorim, I., Antunes-Martins, A. and Sunkel, C. E. (2004). Different spindle checkpoint proteins monitor microtubule attachment and tension at kinetochores in *Drosophila* cells. *J. Cell Sci.* **117**, 1757-1771.
- Maddox, P., Straight, A., Coughlin, P., Mitchison, T. J. and Salmon, E. D. (2003). Direct observation of microtubule dynamics at kinetochores in *Xenopus* extract spindles: implications for spindle mechanics. *J. Cell Biol.* **162**, 377-382.
- Maiato, H., Sampaio, P., Lemos, C. L., Findlay, J., Carmena, M., Earnshaw, W. C. and Sunkel, C. E. (2002). MAST/Orbit has a role in microtubule-kinetochore attachment and is essential for chromosome alignment and maintenance of spindle bipolarity. *J. Cell Biol.* **157**, 749-760.
- Maiato, H., Fairley, E. A. L., Rieder, C. L., Swedlow, J. R., Sunkel, C. E. and Earnshaw, W. C. (2003). Human CLASP1 is an outer kinetochore component that regulates spindle microtubule dynamics. *Cell* **113**, 891-904.
- Maiato, H., Khodjakov, A. and Rieder, C. L. (2005). *Drosophila* CLASP is required for the incorporation of microtubule subunits into fluxing kinetochore fibres. *Nat. Cell Biol.* **7**, 42-47.
- Rogers, G. C., Rogers, S. L., Schwimmer, T. A., Ems-McClung, S. C., Walczak, C. E., Vale, R. D., Scholey, J. M. and Sharp, D. J. (2004). Two mitotic kinesins cooperate to drive sister chromatid separation during anaphase. *Nature* **427**, 364-370.
- Rogers, G. C., Rogers, S. L. and Sharp, D. J. (2005). Spindle microtubules in flux. *J. Cell Sci.* **118**, 1105-1116.
- Sharp, D. J., Rogers, G. C. and Scholey, J. M. (2000). Microtubule motors in mitosis. *Nature* **407**, 41-47.
- Tan, A. L., Rida, P. C. G. and Surana, U. (2005). Essential tension and constructive destruction: the spindle checkpoint and its regulatory links with mitotic exit. *Biochem. J.* **386**, 1-13.
- Taylor, S. S., Scott, M. I., Holland, A. J. (2004). The spindle checkpoint: a quality control mechanism which ensures accurate chromosome segregation. *Chromosome Res.* **12**, 599-616.